Modeling of the thermal performance of piglet house with non-conventional floor system

Débora Caroline Gonçalves de Oliveira, Melissa Selaysim Di Campos, Nady Passé-Coutrin, Cristel Onesippe Potiron, Ketty Bilba, Marie-Ange Arsène, Holmer Savastano Junior

Modeling of the thermal performance of piglet house with non-conventional floor system

Débora Caroline Gonçalves de Oliveira[a], Melissa Selaysim Di Campos[b], Nady Passé-Coutrin[c], Cristel Onésippe Potiron[c*], Ketty Bilba[c], Marie-Ange Arsène[c] and Holmer Savastano Junior[a].

[a] Universidade de São Paulo, FZEA, Núcleo de Materiais para Biossistemas, Avenida Duque de Caixas 225, Pirassununga, São Paulo - Brasil.

debora_zoo@yahoo.com.br, holmersj@usp.br

[b] Universidad Federal de Goias Escola de Veterinária e Zootecnia (EVZ).Rodovia Goiânia-Nova Veneza, Caixa Postal 131Campus Samambaia 74691105 - Goiânia, GO – Brasil

melissa@ufg.br

[c] Université des Antilles, Laboratoire COVACHIM-M2E EA 3592 Campus de Fouillole, UFR SEN, BP 250, 97157 Pointe-à-Pitre Cedex, Guadeloupe – France (F.W.I.)

nady.passe-coutrin@univ-antilles.fr, cristel.onesippe@univ-antilles.fr, ketty.bilba@univ-antilles.fr, marie-ange.arsene@univ-antilles.fr

* corresponding author: cristel.onesippe@univ-antilles.fr Tel : (590)590483217

Abstract.

This work proposes a modeling for the thermal behavior of piglets' house, based on innovative alternatives material and sustainable production systems. The applied finite difference method is applied for the solid system up to the floor and the finite volume method is applied in the piglets' house using the CFD toolbox Open FOAM. Both models simulate each temperature value inside the shelter in order to adjust the thermal floors heating parameters convenient for an optimum animal welfare. The cement based floors were fabricated applying residual materials: swine deep bedding ashes and short sisal fibers. The correlation between modeled and experimental values is satisfactory (standard deviation of 1.37 K for the floor temperature determination and 0.56 K for the black globe temperature determination). The temperature of external environment and inside the piglets' house are effective to adjust the temperature of the electrical resistance of the thermal floor for better performance of the piglets' microenvironment.

Keywords: finite difference method; finite volume method; thermal modeling; fiber-cement composites; swine deep bedding ashes.

1. Introduction

The breeding environment has a direct influence on the thermal comfort and animal welfare, promoting the maintenance of heat balance within the premises, air quality and the expression of their natural behavior, affecting the productive and reproductive performance of the pigs [1-3].

1.1 Thermal comfort in swine production

An assertive determination of the thermal conditions and thermal comfort is more complicated in an environment in which a complexity of thermal factors is operative [4].

One of the biggest problems related to thermal comfort and welfare in pig production is in the maternity ward, because the sows have a thermal comfort zone different of piglets [2]. The control conditions in a small space, where two distinct environments need to be provided, are more complex than in other stages of production. Figure 1 illustrates this installation where the female and her piglets share the space: it is noted that only the piglets have access to the piglets´ house. During their first days of life, the piglets have no effective mechanism to control their body temperature, making it sensitive to the cold environment. The evaluation of the internal microclimate of piglets´ house is important since the control of floor temperature can have a direct influence on the development of piglets [4-12].

The thermal comfort zone for piglets in the first weeks of life (Table 1) is limited by the lower critical temperature (LCT). LCT is the environmental temperature below which the animal activates its thermoregulatory mechanisms to produce heat in order to balance the dissipation of heat to the cold environment. Another temperature of interest is the high critical temperature (HCT), above which occurs thermoregulation in order to assist the animal body heat dissipation to the environment.

As demonstrated in Table 1, the piglets, by their physiological characteristics, have difficulty adjusting to environmental thermal fluctuations. The temperature range for comfort varies with their age. It is necessary to provide external heat sources and some sort of insulating flooring in the shelter area to avoid piglets hypothermia as the temperature is normally kept within the sows' thermal comfort zone, that is to say around 20°C [8, 13-14].

One way to provide thermal comfort to piglets is the use of a shelter heated under lamps or built with special thermal floor warmed by electrical resistances, keeping the comfort temperature for the piglets [15]. When the piglets are heated, they spread on the floor to control their body temperature. If it is too cold, they will huddle or they will lie near or on top of the sow.

1.2 Building materials based on recycled wastes

The requirement of environmental sustainability in animal production represents a considerable challenge to pig producers in recent decades. The type of floor adopted by most of swine producers is a partially or a totally slatted floor, and the production systems require the use of manure deposits or ponds for storage. However, these major investments are not always compatible taking in account the economic reality of this sector in developing countries such as Brazil.

The deep bedding system is an alternative in which the waste composting takes place in the production site in order to reduce the risk of air, water and soil contaminations and to have alternative utilization of the generated residues including better agronomic value. In addition to the application as a fertilizer, alternatives are searched in order to re-use this bed after utilization; for example, there is the possibility of burning it as a biomass for thermal energy generation [10, 16].

The use of the resultant swine deep bedding ashes as pozzolanic material to partially replace ordinary Portland cement in civil construction materials, can lead to energy savings, and assist in the sustainability increase of the production chain [10, 16]. The cement based composites for prefabricated components can be used on those heating floors applied in swine production infrastructure, keeping in mind the recycling of residues generated and also the better quality of the production environment.

The use of vegetable particles and fibers (such as residues from agriculture activity, e.g. sugar cane, sisal and coconut), is also of potential interest for the fabrication of cement based composites, as reinforcing elements or generating voids with lightweight effect due to the entrapment of air in the material.

Several studies [17-20] developed with those industrial and agriculture wastes have demonstrated that the fibers can modify the physical and mechanical macro-structure of the resulting building materials, making them suitable for rural and civil construction in general, including panels as flooring and cladding elements.

1.3 Method for thermal simulation

The thermal simulation can be used for modeling the temperature distribution in the internal environment for example in the adjustment of heating parameters and/or for optimum comfort of the animals.

Based on the concepts previously exposed, the main objective of this work was the proposition of a modeling for the thermal behavior of the piglet's house. A simulated piglets' house has been entirely created. The finite difference method and the finite volume method for the atmosphere inside the shelter were performed to solve the model equations.

The aim of this thermal simulation was to model each temperature value in the interior space of the piglets' house, in order to adjust the heating parameters corresponding to the cement based thermal floor. Then the heating parameters could be adjusted in order to provide better thermal comfort and ideal welfare of the piglets.

2. Materials and methods

2.1 Design and fabrication of cement based thermal floor

The panels were produced with cement composites and used for the fabrication of the thermal floor. The composites are based on cement mortars with 30% substitutions of commercial Portland cement by ashes and with the addition of vegetable fibers. The use of these raw materials with different physical characteristics such as particle size, for example, can favor the packaging effect due to the different morphology.

The main purpose of the ashes was to increase the thermal conductivity of the material and the durability of the vegetable fibers in the long term [21]. The reinforcing fibers were chosen to improve performance for dynamic loads in the initial ages and for creating a significant volume of capillary pores in the materials. The electrical resistance was positioned under the multilayer board and insulated in order to avoid energy losses. A flowchart of the characterization and evaluation carried out in the methodology is presented in Figure 2.

2.1.1 Selection of raw materials for the board fabrication

High early strength Portland cement Brazilian class CPV - ARI (equivalent to ASTM C150 Standards Type III) was used in formulations of cementitious composites to avoid the influence of unknown content of other mineral additions. This type of cement, that achieves high strengths in the initial days of hydration, is recommended in the production of prefabricated elements.

The production based on deep bedding system is an alternative in which the waste undertakes composting "in situ" in order to reduce the risk of pollution of air, water and soil. This system is also recognized to add better agronomic value to the generated waste. In the search for alternatives to the use of this bed, mostly used as fertilizer, there is also the possibility of burning for energy co-generation [22]. Swine deep bedding consists of base or starting material (rice husk in the present study) and dejects generated during the productive cycle, such as urine, manure and feed. Swine deep bedding was collected in the region of Rio Verde, State of Goiás, Brazil (17°47' S; 50°55' W, 715 m altitude above sea level). It was generated from a farm, with pigs in the phase of growth and termination.

The referred bed was used during three consecutive lots of pigs, totalizing 1000 pigs in 360 days of production. Five sub-samples with the same amount (200 g), in five different points were collected. Ashes were produced by calcination of the bedding material in a muffle (Jung brand, model LF10010) with heating ramp of 5°C/min, up to 600°C and kept at this temperature for 3 h, and then cooled naturally.

After burning and cooling steps, these materials were placed in a rotary ball mill (Tecnal / model TE-500) with porcelain jar of 7.5 L of volume capacity, containing 32 balls of porcelain (24-26 mm diameter) at the speed rotation of 200 rpm, during 180 min.

The residual short sisal fibers (used for reinforcement and air entrainment in cement composites) were provided by Sindifibras, Brazil, as part of a collaborative project in partnership with the Agency for Supporting Service for Micro and Small Companies - SEBRAE, Brazil, and the Food and Agriculture Organization (FAO).

The river sand used as aggregate for the cement-based mortar was collected in Pirassununga, State of Sao Paulo, Brazil and was classified as medium coarse sand [23].

2.1.2 Raw material characterization

The samples of swine deep bedding ashes (DBA) and the ordinary Portland cement (OPC) were characterized using the particle size distributions analysis and the respective equivalent diameter of the particles were determined by low angle scattering laser analysis (Malvern brand / model MMS Mastersizer).

Chemical composition and loss on ignition were also carried out. X-ray fluorescence spectrometry was performed using diffractometer Philips, model MDP 1880, for the samples of deep bedding ashes (DBA) and ordinary Portland cement (OPC).

The specific surface area and the helium bulk density of DBA and OPC were determined using a BET (specific surface area) and a helium multipycnometer Quantachrome brand, Ultrapycnometer 100 (specific density).

Sand characterization was performed according to ASTM C136 [23], using a set of sieves (Micolesty brand). The fineness modulus and the maximum diameter of aggregate were calculated following the previously mentioned Standards.

For characterization of the length and thickness of sisal chopped fibres, 50 samples were selected, using the stereomicroscope, Zeiss model Stemi 2000 with magnification lens x 2. The specific density of the sand and sisal fibers were also determined using helium multipycnometer Quantachrome brand, Ultrapycnometer 100.

2.1.3 Composites production and characterization

Cement-based composites materials were elaborated with swine deep bedding ashes (DBA) and reinforced with sisal chopped fibers. The cement-based composites were initially molded in (160 x 160 x 3) mm^3 pads. They were prepared in laboratory using slurry vacuum de-watering process followed by pressing technique, as described by Savastano Jr. et al. [24].

The initial cure for two days was carried out in controlled environment (25 ± 2)°C and (70 ± 5)% of relative humidity; where the composites remained in sealed plastic bags (saturated air at room temperature). After this period, the composites were removed from the bags and immersed in water at room temperature for the following 26 days. After 28 days, the composites were cut in the nominal dimensions of (160 x 40 x 3) mm^3 with water cooled diamond disk, and tested in saturated water condition.

Four mixes of composites were elaborated: (1) Reference as control sample without any mineral addition or fiber reinforcement, (2) (OPC + DBA) with DBA as partial replacement of cement (OPC), (3) (OPC + Sisal) with sisal fibers as reinforcement and (4) (OPC + DBA + Sisal) with both DBA and sisal fibers, as replacement of cement and reinforcing phase respectively. Proportions of mixes are shown in Table 2. The mixtures kept the approximate proportion 1:3 (binder : aggregate). In the case of (OPC + DBA) and (OPC + Sisal) the amount of ashes was considered as part of the binder and the amount of fibers as part of the aggregate phase.

The four composites described above were characterized by helium bulk density testing, isothermal calorimetry and thermal conductivity testing.

The bulk density of the composites was evaluated using helium gas intrusion under helium gas flow with a “Pycnomatic” Thermo Electron Corporation equipment (Les Ulis, France) pycnometer. Five measurements were conducted for each composite at 25°C and relative humidity of 70-80%. Various small pieces of the same composite (3 g, each) were tested as repetitions in order to evaluate the different composite formulations with confidence.

Isothermal calorimetry has been carried out on a C80 calorimeter (Setaram, France); this apparatus is usually utilized to determine specific heat of cement composites exposed to air atmosphere. All samples taken from different composite formulations have been measured at least twice, at 30°C and 70-80% of relative humidity. Prior to the measurements, samples were placed in a desiccator in order to avoid the variation of relative humidity. The C80 calorimeter gives valuable results when the operating temperature is higher than ambient temperature (i.e. 28°C).

Thermal conductivity was measured under controlled laboratory conditions (temperature ~20°C and relative humidity of 70–80%). The apparatus used was a thermal conductivimeter "CT–mètre" with a thermal probe commercialized by Controlab (Saint–Ouen, France) based on transient plane source (TPS) method. Six measurements were conducted for each composite with one-hour interval between each measurement in order to evaluate the standard deviation of the results.

2.1.4 Board production

The formulations used for the production of the multilayer board to piglet's house is described in Tables 2 and 3. Figure 3 is a scheme of the multilayer board and this is a combination of composites (OPC + DBA) (top layer – 1/3 thickness, 1 cm) and (OPC + DBA + Sisal) (bottom layer – 2/3 thickness, 2 cm).

2.2 Construction and instrumentation of the piglets´ house

The floor of the piglets´ house is heated with electrical resistance; the bulb thermostat temperature is maintained in the center of the resistors (at 45°C) for this study. The electrical resistance temperature is kept constant without affecting the analysis of the other variables related to the floor and the environment. The electrical resistance is insulated by ceramic bricks. As the ceramic bricks and the multilayer board have close thermal conductivity values, there is no deformation of the circular isotherms when they cross the interface and then it is assumed that the floor has a uniform temperature.

Figure 4a illustrates the layout of the electrical resistance and the bulb thermostat. Figure 4b shows the multilayer board on its top, as the base for piglets´ house and the Figure 4c is a schematic side sectional indicating to the arrangement of electrical resistances in relation to multilayer board.

To characterize the microenvironment inside the piglets´ house (Figure 5), data-loggers were used (brand Hobo U12-012/ Onset) for collection of the air temperature (AT) and relative humidity (RH) necessary for the determination of the enthalpy (H). Enthalpy (H) is a thermal comfort index that expresses the heat amount in 1 kg dry air, in kJ, determined by the equation (equation 1) cited by Rodrigues [25].

$$H = 6.7 + 0.243AT + \frac{RH.10^{7.5AT/237.3+AT}}{100} \qquad \text{Equation 1}$$

where: H = enthalpy (kcal/kg dry air), AT = air temperature (°C), and RH = relative humidity (%).

The result of this equation is in kcal/kg of dry air and the enthalpy unit is in kJ/kg of dry air, so the value of the equation must be multiplied by 4.18.

Inside the black globe, a data-logger sensor collected the black globe temperature, a way of indicating the combined effects of radiation, convection, and its influence on the animal comfort [26]. Data were collected for 7 days every 15 min by the sensors and were stored in the loggers. The sensors were placed at the geometric center of the piglets´ house because the piglets stay a few weeks in this environment (approximately 21 days) thus the ideal height can vary over that time as the piglet grows and increases weight. The same methodology was adopted for the collection and storage of the external environment data – an open space with a roof cover where the piglets' house was positioned. In this case, the sensors were positioned 30 cm above the roof of the piglets´house (Figure 5).

2.3 Mathematical modeling of thermal behavior

There are two different domains where heat transfer occurs: (1) a solid one from ground to the floor of the piglets' house in which heat transfer may be considered as purely diffusive and (2) a gaseous one i.e. the piglets' house atmosphere limited by the ceiling and the lateral walls, where the heat transfer is mainly a natural convective one.

Working on the coupled phenomena is difficult particularly because of the unsteady aspect of the natural convection inside the piglets' house. The initially very weak gas flow rate and the large experimental gap of temperature between the resistance and the upper layer of the floor lead to consider the floor temperature mainly due to diffusive heat flow from the electrical resistance. That is why we propose to decouple the phenomena study in the following way. The piglets' house is treated by two series of separated conditions.

At first, the multilayer board is heated by the electrical resistance located under the floor. The heat transfer may be considered as purely diffusive to determine the upper floor temperature. The electrical power is adjusted to obtain the required temperature. A Poisson equation (equation 2) is solved using the finite difference method.

$$\nabla^2 T - \frac{1}{a}\frac{\partial T}{\partial t} = \frac{-S_h}{\lambda} \quad \text{Equation 2}$$

where S is the power from resistance (W m^{-3}), a is the diffusivity and λ is the thermal conductivity of the solid medium.

The second part of the simulation is proceeded to obtain the temperature distribution inside the piglets' house. This case is a problem of natural convection because of heating from below. Natural convection on horizontal board, when the surface is warmer than the upper fluid is a particularly complex and often unsteady problem [27]. A solved case is published by Ouertatani et al. [28]. With the temperature gap being smaller than 30 K, the Boussinesq approximation can be used [27]. This approximation is a simplification of Navier-Stokes equations which govern the motion of fluids. It is typically used to model natural ventilation in buildings or dense gas dispersion in industrial set-ups [29]. The first criteria for using this approximation are the following for the concerned gas medium:

- the flow rate is small compared to sound rate (having a small Mach number),
- the gas is considered as perfect and incompressible and
- the viscous dissipation is very weak.

To establish the equations of Boussinesq approximation, a reference thermodynamic state of the fluid (P_0 and T_0) is defined from which the following assumptions are made:

1. The thermo-physical properties of the fluid are supposed to be constant except for the gas density in the gravity term. They are calculated at T_0 and P_0.
2. Only temperature effects on density are considered in the gravity term. Pressure variations effect is neglected.

3. The density is so expressed as $\rho(T) = \rho(T_0)\,[\,1 - \beta\,(T - T_0)]$
4. The work of pressure and viscous dissipation strengths is neglected in the energy equation.

The Navier-Stokes equations are so simplified (equations 3, 4, 5).

$$\vec{\nabla}.\vec{u} = 0 \qquad \text{Equation 3}$$

$$\frac{\partial \vec{u}}{\partial t} + \left(\vec{u}.\vec{\nabla}\right)\vec{u} = -\frac{1}{\rho}\vec{\nabla}p + \nu\nabla^2\vec{u} + \beta\left(T - T_0\right)\vec{g} \quad \text{Equation 4}$$

$$\frac{\partial T}{\partial t} + \vec{u}.\vec{\nabla}T = a\nabla^2 T + \frac{S}{\rho C_p} \qquad \text{Equation 5}$$

The two unknown parameters are $\vec{u}$ the flow rate vector and T the temperature.

$\vec{g}$ is the gravity vector, a is the thermal diffusivity of the gas, C_p the thermal capacity at constant pressure, ρ the gas density.

A finite volume method is used to discretize the Navier-Stokes equations to find the flow rate and energy equation to get the temperature. This work is done using OpenFOAM, the open source CFD (computational fluid dynamics) toolbox [30].

2.3.1. Modeling heat transfer up to the floor

Up to the floor, the energy equation for the steady state heat diffusion conditions is the following (equation 6) according to the Fourier law of conduction.

$$\nabla^2 T = -\frac{S}{\lambda} \qquad \text{Equation 6}$$

S is the volumetric rate of heat generation (or power source), λ is the medium thermal conductivity and T is the temperature to be determined.

The calculus domain is a box 200 cm large x 200 cm deep x 200 cm high and the piglets' house (60 cm large x 80 cm deep x 50 cm high) is put on the base and centered in the domain. The piglets' house floor of 3 cm thick and the resistance under the floor (already described in section 2.2.) are outside the calculus domain. The piglets' house has a unique opening.

The boundary conditions are as exposed below:

- Static atmosphere and steady state,
- External temperature is situated on the limits of the calculus domain,
- S, the rate of heat generation value is different from zero at the heating sources positions. The unique sources are two parallel electrical resistances positioned under the multilayer board.

The entry data, which have to be modified when changing experimental case, are the external temperature and the thermal conductivity for the multilayer board. The fixed entry data are all the dimensions and the thermal conductivities of each layer of the floor and under the floor materials (Table 4).

The finite differences method is used for equation solving. The maximum number of iterations is one thousand and the tolerance for the solving of this linear system is 10^{-12}. The results of this simulation give the floor temperature.

2.3.2. Modeling of thermal behavior inside the piglets' house.

The calculus domain is the piglets' house atmosphere. Because of the form below heating thermal convection is the main type of heat transfer. It is a case of Rayleigh-Bénard convection because the Rayleigh number, comparing Archimède and viscosity strengths, is about 10^8. The criterium for occurring of this convection type is a Rayleigh number larger than 1708 [31].

The used calculus code, OpenFOAM (version 3.0.1) provides a tutorial near for the present case, "hotRoom" from "buoyantBoussinesqPimpleFoam" for transient conditions, in the larger directory "heatTransfer". The difference lies in the searched parameter that is to say the pressure for the described case. The case is transformed to put temperature parameter as first researched parameter. The geometry is modified and the new boundary conditions are created.

The boundary conditions are as exposed above. External meteorological temperature (T_{ext}) is on the ceiling and practically on the lateral walls of the house. The multilayer board temperature (T_{floor}) is an initial and constant datum.

The finite volume method requires a mesh which is refined up to 40 cells on x direction (large), 40 cells on the y direction (deep) and 80 cells on z direction (high), because the temperature gap is in that direction.

The initial temperature for the atmosphere inside the house is fixed at T_{ext}. The software is run for times chosen from 600 to 3600 s (six values). So the hot resistance is supposed to be switched on time zero.

The first results are the black globe temperatures, above the center of the multilayer board at 30 cm height. From the number and position of each cell of the mesh (128000 cells inside the house) the black globe mesh cell number is deduced: 68032.

Because of the fact that the resistance is switched on the whole day, the external temperature varies and the six simulation results are next to each other; experimental value is compared to the mean value of the six simulation results. The period considered with the lowest temperatures of the day was chosen for the study: from 8 PM to 6 AM next day. The second results are the field of temperature in the piglets' house.

3. Results and discussion

3.1 Raw material characterization

3.1.1 Ordinary Portland cement

The particle size distribution of Portland cement is depicted in Figure 6. The values for D50 (particle diameter in µm, at 50% of cumulative distribution) and D90 (particle diameter in µm at 90% of cumulative distribution) are, respectively, 10.11 µm and 30.23 µm.

The specific surface area and the specific density of cement are 0.98 m^2/g and 3.10 g/cm^3 respectively. Chemical composition of Portland cement is reported in Table 5. The chemical composition of ordinary Portland cement is in accordance with the specifications of ASTM C150 [32] and NBR 16697 [33].

3.1.2 Swine deep bedding ashes

The calcined ashes presented average diameter of 20.7 µm. The broad particle size distribution (Figure 7) demonstrates the heterogeneous origin of these ashes as they can contain a variety of constituents with different hardness to crushing in the milling process. D50 and D90 of the ashes are, respectively, 17.24 µm and 42.59 µm.

Chemical composition and loss on ignition of swine deep bedding ashes are presented in Table 5. The amount of SiO_2 in swine deep bedding ashes (47.9 wt%) is comparable with the value (45.1 wt%) obtained by Di Campos et al. [16]. This high value of SiO_2 is one of the premises for considering the material as pozzolanic [34]. Additionally the sum of (SiO_2 + Al_2O_3 + Fe_2O_3) was equal to 68.2 wt% what is acceptable for the inference of pozzolanic character of the ashes, according to ASTM C618 [35] the minimum acceptable value being 50%. The value of loss on ignition of 6.5 wt% can be explained by the remaining of uncalcined material. After burning at 600°C, the specific density of the swine deep bedding ashes was determined as 2.95 g/cm^3.

The X-ray diffractogram of DBA is shown in Figure 8. An amorphous halo can be identified in the interval between 2θ from 20° and 40° what is a clear indication of the presence of amorphous phases. Some crystalline phases were also detected, and they can be related to the presence of quartz and other impurities in these residual ashes.

3.1.3 Sand and sisal fibers

The maximum diameter of sand was equal to 2.42 mm and fineness modulus was 2.20 mm being therefore classified as medium sand, according to ASTM C70 [36]. The specific density of the sand was 2.60 g/cm^3 and the real density was 1.60 g/cm^3.

The residual sisal fibers have an average length of 23 mm and thickness of approximately 500 μm, the specific density was 1.40 g/cm^3. The size and thickness of the fibers can also affect the porosity and the thermal performance of the matrix [21]. These values are lower than the length indicated by Joseph et al. [17] and Yang Li et al. [37]. The fiber length plays a major role in the load transferring with the matrix;

however, greater lengths can prejudice the homogeneous distribution of the reinforcing elements.

3.2 Composites characterization

3.2.1 Helium bulk density

Figure 9 summarizes the results of helium bulk density measurements by pycnometry tests. For the studied formulations the addition of ashes and/or fibers significantly affects the values of helium bulk density for (OPC + DBA) and (OPC + DBA + Sisal). Specific density of swine deep bedding ashes is about 2.95 g/cm^3 that is to say lower than the cement density (which is 3.10 g/cm^3). Thus, according to a simple law of mixtures, (OPC + DBA) has a lower value of helium bulk density than Reference, because cement is partially replaced by a lighter material (DBA). The highest value of helium bulk density of (OPC + DBA + Sisal), when comparing with (OPC + Sisal), could be explained by the fact that the synergistic presence of ashes and fibers decreases the voids in the composite. Indeed, as cement and ashes present a similar size distribution (see Figures 6 and 7), ashes probably fill a large part of the pores of cement [38]. Consequently, there is a densification of the sample.

When comparing helium bulk density of Reference and (OPC + Sisal), a very little difference is observed because partial replacement of sand by sisal fibers is low.

3.2.2 Specific heat

Specific heat of a material represents its capacity to retain heat. Thus, a high specific heat is required due to the associated ability to retain heat in piglets' house [39]. As explained by Castro Mendes et al. [40], specific heat of a substance relates to the manner in which the internal energy of its constituents is distributed.

Generally, it is observed in Figure 10, the denser the material, the higher the specific heat. According to standard deviation of specific heat, a significant difference is observed only between OPC + DBA and the 3 others. Indeed, the specific heat of Reference i.e. without any replacement is 230 J/kg K, it is quite the same for (OPC + Sisal) and for (OPC + DBA + Sisal), and (OPC + DBA) has a specific heat around 110 J/kg K. This value is significantly lower than reference by factor 2 (Figure 10). This is compatible with the lower helium bulk density of (OPC + DBA) as depicted in Figure 9 and is probably associated to the air entrapment by the ashes during the mixing procedures.

Replacement of around 30% by mass of OPC by DBA leads to a cementitious material, which retains twice less heat than the reference. The partial replacement of cement by DBA seems to be more influent on specific heat than replacement of cement by vegetable fibers. In literature, when adding fibers to cement, it is observed an increase of specific heat of matrix [41]. This fact is observed when comparing (OPC + Sisal) and Reference, taking into account the standard deviation. As explained by Ratiarisoa [38] and above, cement and ashes having similar particle sizes, ashes, when they are combined with vegetable fibers, act like a filler and lead to a densification of matrix. This densification and the combined effect of fibers is probably the reason why (OPC + DBA + Sisal) exhibits a higher specific heat than Reference. The high standard deviations of samples (OPC + Sisal) and (OPC + DBA + Sisal) is probably related to the elaboration process.

3.2.3 Thermal conductivity

Figure 11 presents the thermal conductivity of the composites. Thermal conductivity represents how a heat flow progresses through the material. A low thermal conductivity is required to have an insulating material [42].

Thermal conductivity of Reference is (1.082 ± 0.032) W/m K whereas thermal conductivities of (OPC + DBA), (OPC + Sisal) and (OPC + DBA + Sisal) are respectively (0.809 ± 0.037) W/m K, (1.200 ± 0.092) W/m K and (0.761 ± 0.081) W/m K.

The lowest values for thermal conductivity are linked to (OPC + DBA) and (OPC + DBA + Sisal) and they seem to be related to the presence of deep bedding ashes in the formulations. This behavior can be understood, as explained by Castro Mendes et al. [43], by the amount of entrapped voids in the specimen. The DBA is an amorphous porous material, and organic compounds of sisal promote the reduction of thermal conductivity [44].

In comparison with Reference, the more remarkable insulating effect is obtained with (OPC + DBA + Sisal) when both ashes and fibers are present in the cement matrix.

According to the standard deviation, (OPC + Sisal) has the same thermal conductivity as Reference. The vegetable fibers have a lower conductivity than the mineral matrix so the cement matrix incorporating vegetable fibers should have lower thermal conductivity than pure matrix [45]. The similarity of thermal conductivities of Reference and (OPC + Sisal) could be explained by the poor/lack of control of moisture content / relative humidity and / or water absorption during the elaboration of (OPC +

Sisal), which would also explain the abnormally high helium bulk density of this sample (Figure 9) [46].

There is a compromise between the energy efficiency of the heating system and the thermal conductivity of the floor panel. If the thermal conductivity of the floor is too high, it can burn the skin of the piglets. On the other hand, if the thermal conductivity is too low, the heating resistances will have to reach higher temperatures to keep the piglets at a desired comfortable temperature and, thus, consuming more energy. In this case, heat will be concentrated close and right above the resistance. Further studies would be necessary to find an ideal thermal conductivity for the system (heating resistances x multilayer board x piglets comfort).

3.3 Evaluation of the internal environment

Based on the results obtained in the characterization of the raw materials combined with those of the composites, one multilayer board was selected for the assessment of the environment in the piglets´ house and validation of the mathematical modeling. The multilayer board is a combination of the composites (OPC + DBA) (top layer – 1/3 thickness, 1 cm) and (OPC + DBA + Sisal) (bottom layer – 2/3 thickness, 2 cm).

3.3.1 Air parameters of the internal environment

To calculate the enthalpy (H), the air parameters (dry bulb temperature and relative humidity of the microclimate inside piglets' house) were considered for the experimental period constituted of four days. These calculated values for enthalpy in the studied period follow in Table 6 and need to be evaluated in comparison with the recommendations listed by Table 1 for thermal comfort zone and relative humidity near 70% preconized for the initial weeks of piglets' life.

According to these data, the comfort levels are not achieved in the periods under observation, however it is important to note that the values are within the range between the comfort temperature and the critical low temperature.

3.3.2 Validation of the model using experimental data

The modeling is carried out in order to:

- fit the floor temperature, and the black globe (BG) temperature at 30 cm from the floor, in the same vertical at night (from 8 PM until 6 AM next day) and
- simulate the whole temperature field in the house.

The experiments are conducted when there is no sunshine. So, the unique heat sources are the two parallel resistances under the multilayer board. Ceramic bricks are on both sides of the resistances giving a large area for the multilayer board to be warmed on the whole. Ceramic bricks and multilayer board have thermal conductivities of close values. This fact allows that the board to be considered at a homogeneous temperature.

One dimension solving has been considered for the heat transfer equation, because of the shape of the heat sources; we use the radius of cylindrical coordinates can be used, allowing examining temperatures above and around the resistances. In the first part of the modeling, the value of the multilayer board temperature is expected but the two heat sources are thin. The ceramic bricks have thermal conductivities as large as the multilayer board one, so they give a large area to warm the multilayer board by contact, allowing getting better simulation results. The wood board is not able to prevent heat loss; this is the purpose of the ground.

For the first part of the simulation (consisting of the research of the floor temperature), the piglets' house floor and under the floor are computed in the large domain (200 x 200 x 200) cm^3 with all the experimental details adopted from the multilayer board developed in the present work. The thermal conductivity was assumed as 1.03407 W/ m K and the temperature of electrical resistance as 45°C (Figure 5).

The pure diffusive heat transfer in solid materials for steady state conditions allows to considering a constant heat flow from the ground to the floor, and the result is the floor temperature. The domain limits are at external temperature.

A first validation of this model is conducted by calculation of the distance between the ground and the resistance plane and then by comparison of calculated and experimental distances, with the external temperature 18.5°C.

The best fit between the experimental and simulated floor temperature is obtained for a distance of 7.5 cm (Table 7).

In this way, the first part of the simulation, applies Fourier's law of conduction at steady state. For the openFOAM development, which is a natural convection problem, more theoretically hard, showed that the gap is not too large if some simplifications about walls temperature (particularly) are made.

Then the running and comparison with experiment of the model are carried out for four other experiments. Table 8 shows the entry of external temperatures and the corresponding dates. The gap between T modeled (M) and T (E) is up to 1.7°C.

If one considers 32°C as the temperature necessary to piglets, this temperature is reached by the experiments and is well fitted by the model. However, the heat transfer into the piglets' house atmosphere is computed by the second part of the simulation, using a CFD toolbox. The entry data are the external temperature and the floor temperature, which are experimental data. The interest of the model here is to be able to follow the temperature in the whole space occupied by the piglets´ body, and to evaluate if the decrease of this temperature is not too negative for their comfort.

The results give the black globe temperature for validation with experimental data. Figure 12 gives the black globe temperatures for a same hour (11 PM) each day and Figure 13 shows the black globe temperatures for two whole nights.

Simulation results are close to experimental ones taking into account the precision. All the six simulated temperatures are successive values. The sensor of the temperature capture seems to see the mean of the temperatures. The enormous gap of temperature next to the floor is the particularity of the natural convection phenomenon (Figure 14). The high temperature stays very close to the floor.

3.3.3 Adjustment of the parameters for optimum conditions of the internal environment for animals' welfare.

The first part of the model is validated with the floor experimental temperature and the second part of the simulation is validated with black globe temperature. The whole temperature field is shown in Figure 14, drawing isothermal lines in the transient state at 3600 s and external temperature equals to 293 K (20°C); The isothermal lines give the range of black globe temperature : 23.5-22.8°C.

The hot temperature is very close to the floor and the Rayleigh-Bénard instability shows convection rolls : the temperature is around 296 K (23°C) in the whole shelter. The piglets can feel 32°C if they are directly on the floor and gathered to keep the necessary heat in the bottom of the shelter (left on Figure 14), far from the opening. It is possible to see the opening of the shelter on the right (blue isotherms) where the temperature is the coldest. At the bottom of the shelter, on the left, there is the best comfort zone for the piglets (white and some red isotherms).

To reduce the gap between floor and black globe temperatures, it would be interesting to add an equation simulating the variations of temperature along the walls, because of the warm floor. It would be also interesting to develop the work by increasing the pixels number for the grid, allowing more precise results.

The piglets' house architecture is simple: it has only an opening for the animals' entrance or exit and the walls/roof are made of wooden 3 cm thick boards. The drop of the experimental temperature from the floor to the roof explains why we have considered the roof temperature does not change significantly. The piglets' house is in a large wooden building: we choose to center it in a building with small openings that is to say small airflow for simulation. In this way, the heat exchanges are supposed to be small from the other envelope structures.

4. Conclusions

A non-conventional system, satisfying sustainable development and better waste management objectives, has been develop for the production of a "piglet house" to increase welfare of the newborn animals. The innovative element for the floor was made from swine deep bedding ashes (DBA) as cementitious material in cement paste (OPC

+ DBA) or in cement composite (OPC+ DBA + Sisal). Indeed, DBA increased the porosity: closed porosity (OPC + DBA) and open porosity in (OPC+ DBA + Sisal), and consequently modify the density of the material and decrease the thermal conductivity of the material.

Inside the shelter, during the studied critical periods, comfort levels remained within the minimum critical temperature necessary to comfort for the piglets, with values above the lower critical temperature.

The aim of thermal modeling was to simulate each temperature value in the piglets' house space, in order to be able to adjust the heating parameters for the best comfort of the just born animals. When outside temperature is 20°C, the temperature, in the shelter, ranges from 34°C on the floor to 23°C (gap of 11°C), where the piglets are gathered. This gap of temperature is considered excessive for the welfare of the animals. A minimal temperature of 28°C would be targeted. To reach this value, a better insulation in the walls and the roof, that is to say smaller conductivities, would be recommendable. A good humidity of the air improves its conductivity value i.e. a smaller humidity is able to decrease thermal conductivity.

- Evaluation of the thermal modeling

The correlation between model and experiment is acceptable (standard deviation of 1.37 K for the floor temperature determination and 0.56 K for the black globe temperature determination), but it can be noticed that the decrease of the temperature is a bit larger for the model than for the experiment, perhaps due to neglecting radiation. The stable gap (around 1.5°C for the different experimental days) allows thinking about other reasons such as the complexity of the dispositive under the floor (i.e. bricks, metal around the resistances, and presence of air in the middle).

- Evaluation of the optimal conditions for the pig production

The proposed model helps in making the decision first step with the material thermal parameters and the external temperature as entry data, the modeling results allowing the adjustment of temperature for better performance of the internal microenvironment of the shelter.

Acknowledgements:

The authors thank:

- Professor Jacques H. Laminie from LAMIA laboratory (Université des Antilles) and Dr François Bade from LaRGE laboratory (Université des Antilles) for their help for modeling statement and calculation,
- Computation Center C3I (Université des Antilles),
- Agence Nationale de la Recherche Blanc Inter II for technical support. SIMI9 décision n° ANR-12-ISO9-0002-01,
- Fundação de Amparo à Pesquisa do Estado do São Paulo, Process n. 2012/51467-3 (ANR FAPESP) and CNPq Brazil (Process n. 307723/2017-8, Research Grant).

References

[1] L.E. Carvalho, S.M.P. Oliveira, S.H.N. Turco, The utilization of nebulization and forced ventilation on the performance and skin temperature of swines in the termination phase. R Bras Zootec 33 (2004) 1486-1491. (In Portuguese)

[2] R. Schormann, S. Ho, Effects of room and nest temperature on the preferred lying place of piglets--A brief note. Appl Anim Behav Sci 101 (3-4) (2006) 369-374. https://doi.org/10.1016/j.applanim.2006.02.003

[3] G.T. Sales, E.T. Fialho, T. Yanagi, R.T.F. Freitas, V.H. Teixeira, R.S. Gates , G.B. Day, Thermal environment influence on swine reproductive performance. In International Commission of Agricultural Engineering (CIGR), (2008) Institut fur Landtechnik.

[4] V. Kotrbacek, The effect of changes in the complexly defined thermal environment on body and skin temperature and energy metabolism in piglets. Acta Vet Br 53 (1984) 31-39. https://doi.org/10.2754/avb198453010031

[5] D. Berthon, P. Herpin, J.L. Le Dividich, Shivering thermogenesis in the neonatal pig. J. Therm. Biol. 19 (1994) 413–418. https://doi.org/10.1016/0306-4565(94)90040-X

[6] P. Herpin, M. Damon, J.L. Dividich, Development of thermoregulation and neonatal survival in pigs. Livest. Prod. Sci. 78 (2002) 25–45. https://doi.org/ 10.1016/S0301-6226(02)00183-5

[7] I.L. Andersen, G.M. Tajet, I.A. Haukvik, S. Kongsrud, K. Bøe, Relationship between postnatal piglet mortality, environmental factors and management around farrowing in herds with loose-housed, lactating sows. Acta Agric Scand 57 (2007) 38–45. https://doi.org/10.1080/09064700601159626

[8] G. Vasdal, M. Glaerum, M. Melisová, K.E. Boe, D.M. Broom, I.L. Andersen, Increasing the piglets' use of the creep area - A battle against biology? Applied Animal Behaviour Science 125 (2010) 96-102.

[9] G. Vasdal, I. Morgedal, K.E. Boe, R. Kirkden, I.L. Andersen, Piglet preference for infrared temperature and flooring. Applied Animal Behaviour Science 122 (2010) 92-97. https://doi.org/ 10.1016/j.applanim.2009.12.008

[10] D.C.G Oliveira, M.S. Rodrigues, S.F. Santos, H. Savastano Jr, Characterization and use of swine deep bedding ashes in cementitious composites. Agricult Eng J 32 (2012) 810-821.

[11] R. Krummer, A.D. Gonçalves, R.T. Lippke, B.M.F.P.P. Marques, T.J. Mores, Factors that influence the performance of piglets in the nursery phase.Acta Scientiae Vet 37-1 (2009) 195-209. (In Portuguese)

[12] D.C.G. Oliveira, V.C. Correia, C.G. Lima, S.R. Oliveira, H. Savastano Junior, Evaluation of the internal microclimate of piggy´s houses with different types of floors. In: Ninth International Livestock Environment Symposium (ILES IX), 2012, Valencia, Espanha. Ninth International Livestock Environment Symposium Proceedings, 2012.

[13] E.M. Baxter, A.B. Lawrence, S.A. Edwards, Alternative farrowing systems: design criteria for farrowing systems based on the biological needs of sows and piglets. Int J of Anim Biosci, 5 (2011) 580-600. https://doi.org/ 10.1017/S1751731110002272

[14] J. Svendsen, L.S. Svendsen, Intensive (commercial) systems for breeding sows and piglets to weaning. Livest. Prod. Sci.49 (1997) 165-179. https://doi.org/10.1016/S0301-6226(97)00012-2

[15] J. Sarubi, L.A. Rossi, D.J. Moura, R.A. Oliveira, E. David, Use of electricity in different heating systems for weaned piglets. Eng Agríc 30 (2010) 1003-1011. http://dx.doi.org/10.1590/S0100-69162010000600002 (In Portuguese)

[16] M.S. Di Campos, N.P. Barbosa, H. Savastano Jr., Swine deep bedding ashes as a mineral additive for cement based mortar. Sci. Agric 65 (2008) 109-115.

[17] P.V. Joseph, J. Kuruvilla, T. Sabu, Effect of processing variables on the mechanical properties of sisal-fiber-reinforced polypropylene composites. Comp Sci Technol 59 (1999) 1625-1640. https://doi.org/10.1016/S0266-3538(99)00024-X

[18] C.M.R. Dias, H. Savastano Jr, M.E.S. Taqueda, V.M. John, Mixture screening design to choose formulations for functionally graded fiber cements. Mat Sci Forum 631-2 (2010) 65-70. https://doi.org/10.4028/www.scientific.net/MSF.631-632.65

[19] C. Onésippe, N. Passé-Coutrin, F. Toro, S. Delvasto, K. Bilba, M.-A. Arsène, Sugarcane bagasse fibres reinforced cement composites: thermal considerations. Comp Part A 41 (2010) 549-556. https://doi.org/ 10.1016/j.compositesa.2010.01.002

[20] A. Guzman, C. Gutiérrez, V. Amigó, R. Mejíade Gutiérrez, S. Delvasto Pozzolanic evaluation for the sugar cane straw. Materiales de Construcción, 61 (2001) 213-225. (In Spanish)

[21] H. Savastano Jr, V.M. John, V. Agopyan, O.P. Ferreira, Weathering of vegetable fibre-clinker free cement composites. Materials and Structures, Cachan France 35 245 (2002) 64-68. https://doi.org/ 10.1007/bf02482092

[22] D.C.G. Oliveira, M.S. Rodrigues, S.F. Santos, H. Savastano Junior, Characterization and use of swine deep bedding ashes in cementitious composites. Eng. Agric 32 (2012) 810-821. https://doi.org/10.1590/S0100-69162012000500001.

[23] American Society for testing and materials – ASTM C136 (2014). Standard Test Method for Sieve Analysis of Fine and Coarse Aggregates. West Conshohocken.

[24] H. Savastano Junior, J. Fiorelli,S.F. Santos, Sustainable and Nonconventional Construction Materials using Inorganic Bonded Fiber Composites. 1. ed. Duxford: Elsevier 1 (2017) 494p.

[25] V.C. Rodrigues, I.J.O. Silva, F.M.C. Vieira, S.T. Nascimento, A correct enthalpy relationship as thermal comfort index for livestock. Int J of Biometeorology 55 (2010) 455-459.

[26] T. Bedeford, C. Warne, The globe thermometer in studies of heating and ventilation. J of Hyg 34 (1934) 458-473.

[27] J.F. Sacurada, Thermal transfers; Initiation and Detailing, Lavoisier (2005) TEC & DOC, Paris. (In French)

[28] N. Ouertatani, N. Ben Cheick, B. Ben Baya, T. Lili, Numerical simulation of two-dimensional Rayleigh-Bénard convection in an enclosure. C. R. Mécanique, 336 (2008) 464-470.

[29] COMSOL Multiphysics: the platform for Physics-based Modeling and Simulation www.comsol.com

[30] 2004-2016 OpenCFD Ltd (ESI Group) www.openFOAM.org

[31] E. Guyon, J.P. Hulin, L. Petit, Hydrodynamique physique. EDP Sciences (Les Ulis), 2001 CNRS Editions (Paris)

[32] American Society for testing and materials – ASTM C 150 (2011). Standard Specification for Portland Cement. West Conshohocken.

[33] Brazilian association of technical standards - NBR 16697 (2018). Portland cement – Requirements, Rio de Janeiro. (In Portuguese)

[34] M.P. Oliveira, A.F. Nobrega, M.S. Di Campos, N.P. Barbosa, Study of calcined kaolin as a partial substitute of Portland cement. Brazilian Conference on Nonconventional Materials and Technologies: Low-cost housing and infrastructure.

Brazil - NOCMAT 2004, Pirassununga. Proceedings. Pirassununga: USP. (In Portuguese)

[35] American Society for testing and materials – ASTM C618 (2003). Standard specification for coal fly and raw or calcined natural pozzolan for use as a mineral admixture in concrete, West Conshohocken.

[36] American Society for testing and materials – ASTM C70 (2006). Standard Test Method for Surface Moisture in Fine Aggregate. West Conshohocken.

[37] L. Yang, M. Yiu-Wing, Y. Lin, Sisal fibre and its composites: a review of recent developments. Comp Sci Technol 60 (2000) 2037-2055. https://doi.org/10.1016/S0266-3538(00)00101-9

[38] V. Ratiarisoa, Valorisation de résidus agroindustriels comme matériaux dans l'habitat et la construction : utilisation de la bagasse dans les liants composés minéraux et les composites, 2018. PhD thesis, Université des Antilles

[39] D.D.L.Chung, Cement-matrix composites for thermal engineering. Appl therm Eng, 21 (2001) 1607-1619. https://doi.org/10.1016/S1359-4311(01)00043-6

[40] J. Castro Mendes, R.R. Barreto, A.S. Santana Castro, G. J. Brigolini, R.A. Fiorotti Peixoto, Factors affecting the specific heat of conventional and residue-based mortars. Constr. Build. Mat. 237 (2020) 117597. https://doi.org/10.1016/j.conbuildmat.2019.117597

[41] D.D.L. Chung, Cement reinforced with short carbon fibers: a multifunctional material. Composites B 31 (2000) 511-526. https://doi.org/10.1016/S1359-8368(99)00071-2

[42] L. Rodier, K. Bilba, C. Onésippe, M.-A. Arsène, Utilization of bio-chars from sugarcane bagasse pyrolysis in cement-based composites. Ind. Crop. Prod 141 (2019) 111731. https://doi.org/10.1016/j.indcrop.2019.111731

[43] J. Castro Mendes, R.R. Barreto, A.C. Barbieri de Paula, F. Pereira da Fonseca Elói, G.J. Brigolini Ricardo, A. Fiorotti Peixoto, On the relationship between morphology and thermal conductivity of cement-based composites. Cem Conc. Comp 104 (2019) 103365. https://doi.org/10.1016/j.cemconcomp.2019.103365

[44] N. Burger, A. Laachachi, M. Ferriol, M. Lutz, V. Toniazzo, D. Rush, Review of thermal conductivity in composites : Mechanisms, parameters and theory. Progress in Polymer Science 61 (2016) 1-28. https://doi.org/10.1016/j.progpolymsci.2016.05.001

[45] Z. Kammoun, A. Trabelsi, Development of lightweight concrete using prickly pear fibres. Construction and Building Materials 210 (2019) 269-277. https://doi.org/10.1016/j.conbuildmat.2019.03.167

[46] L. Boukhattem, M. Boumhaout, H. Hamdi, B. Benmahou, F. Ait Nouh, Moisture content influence on the thermal conductivity of insulating materials made from date palm fibers mesh. Construction and Building Materials 148 (2017) 811-823. https://doi.org/10.1016/j.conbuildmat.2017.05.020

Figure 1:

Fig. 1: Maternity area, showing the female with the piglets. The piglet's house is located in the right side of the image (red arrow)

Figure 2:

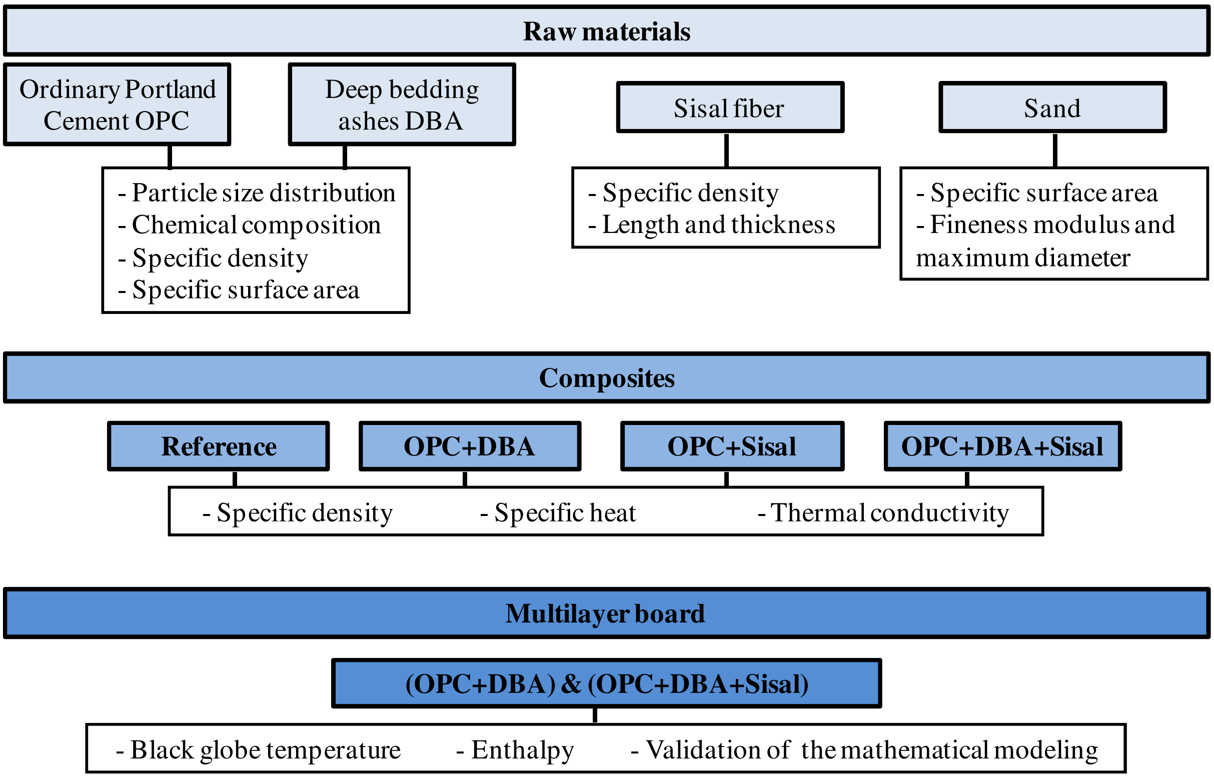

Fig. 2: Flowchart with the characterization for the raw materials, composites and multilayer boards; and validation of the mathematical modeling for the floor board.

Figure 3:

*OPC = Ordinary Portland Cement, DBA = deep bedding ashes, Sisal = sisal fiber.

Fig. 3: Schematic cross-section of the selected multilayer board: (OPC + DBA) & (OPC + DBA + Sisal)

Figure 4:

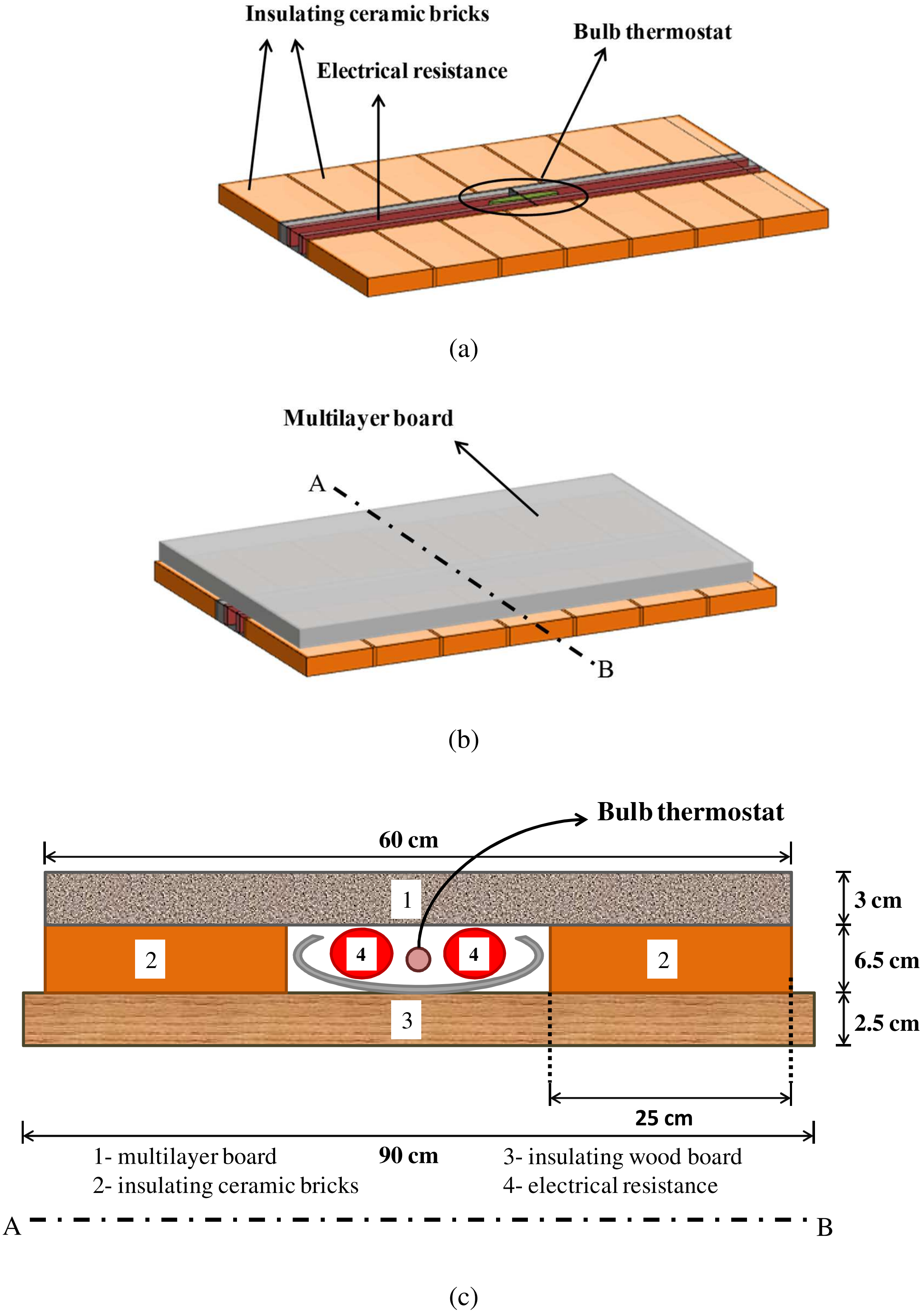

Fig. 4: Drawing (not to scale) of electrical resistance showing the location of the bulb thermostat (a), the multilayer board for the piglets´ house (b), cross-section A-B illustrating the layout of the electrical resistance and multilayer board (c).

Figure 5:

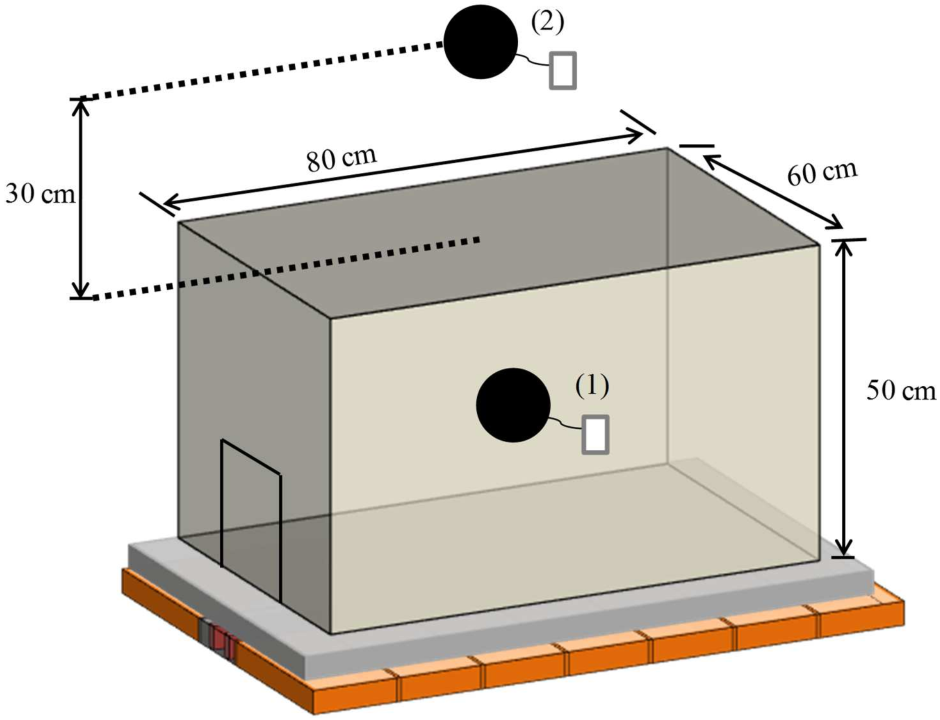

Fig. 5: Image (not to scale) of the sensor for black globe temperature and data-logger in the geometric center of the piglets´ house (1) and above of the piglets´ house (2).

Figure 6:

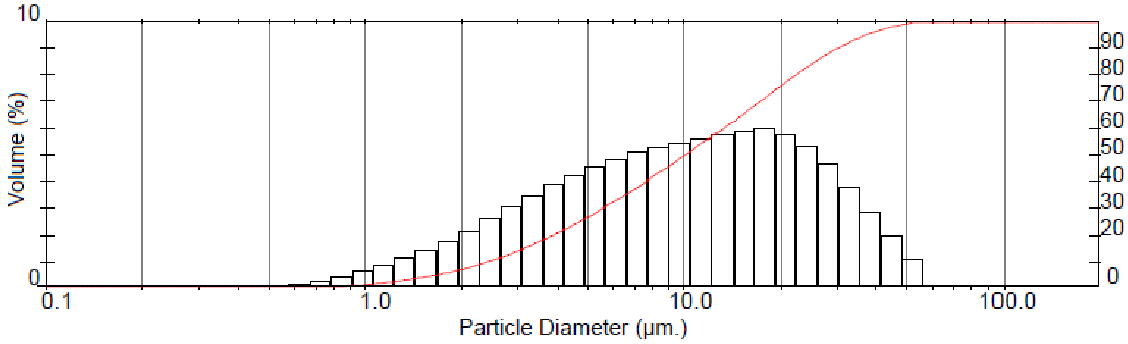

Fig. 6: Particle size distribution of the ordinary Portland cement (OPC)

Figure 7:

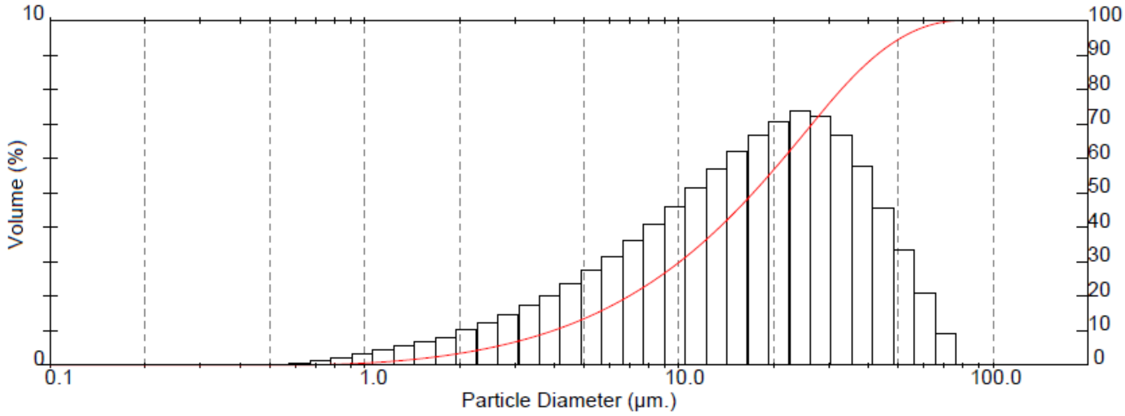

Fig. 7: Particle size distribution of the swine deep bedding ashes (DBA)

Figure 8:

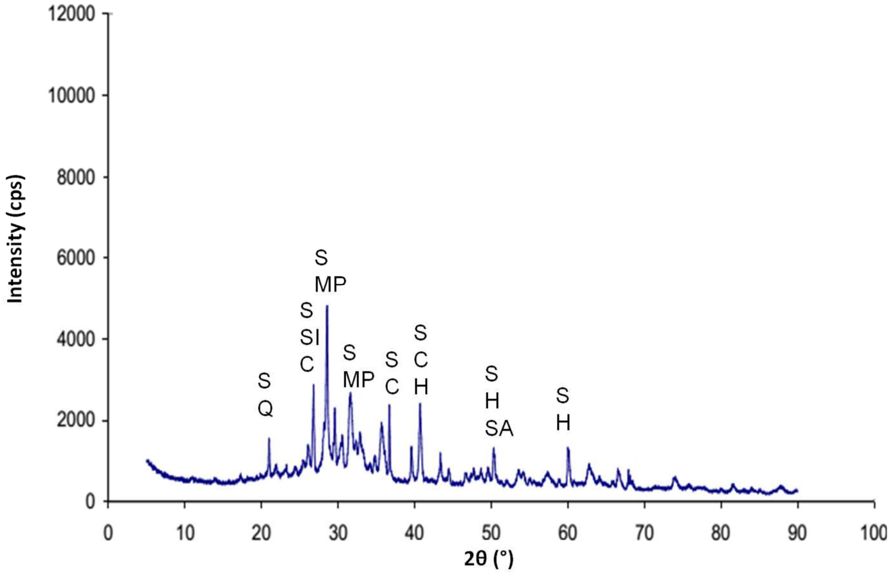

*Crystalline phases: Q - Quartz (SiO_2); MP - Magnesium Phosphate ($Mg_2P_2O_7$); SA - Sodium Aluminium Silicate ($Na_{1,45}Al_{1,45}Si_{0,55}O_4$); SI - Sodium Iron Sulfate ($Na_6Fe(SO_4)_4$), H - Hematite (Fe_2O_3), C - Coesita (SiO_2); S - Sylvite (KCl)

Fig. 8: Diffractogram of swine deep bedding ashes (DBA)

Figure 9:

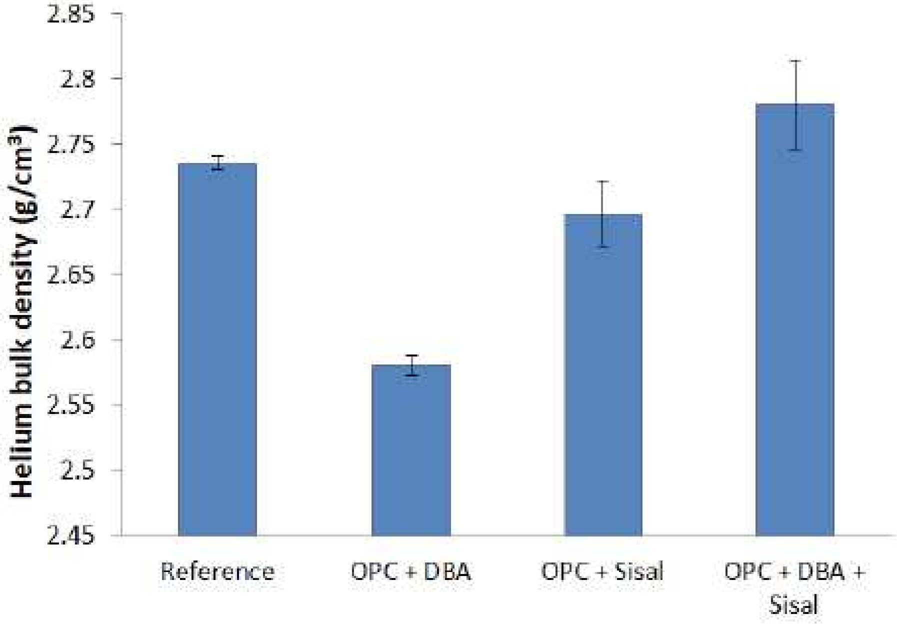

Fig. 9: Helium bulk density (mean values and standard deviations) of the different composite mixtures

Figure 10:

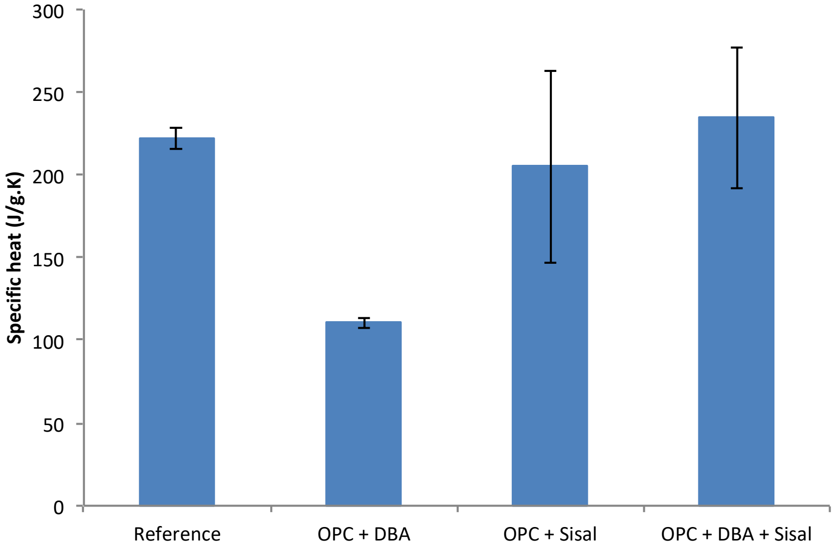

Fig. 10: Specific heat of the different composite mixtures

Figure 11:

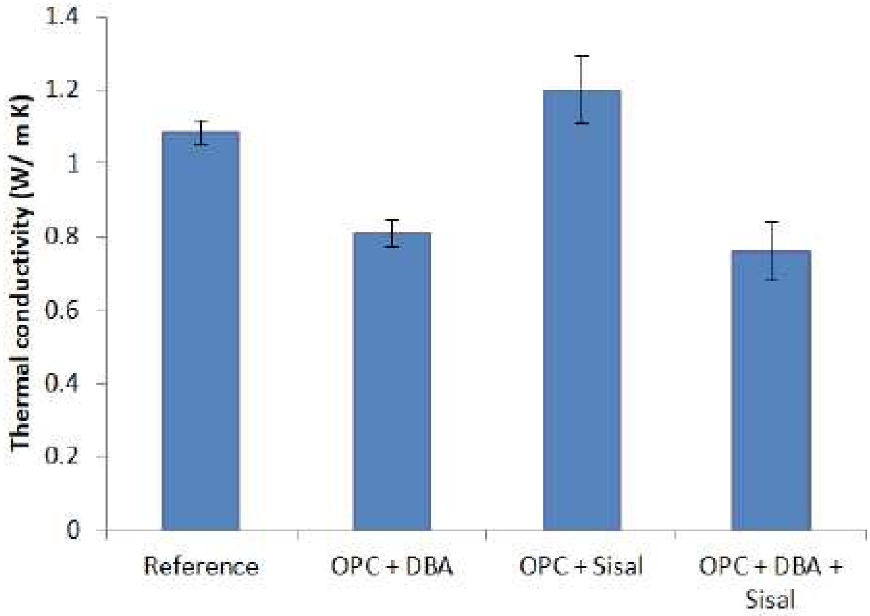

Fig. 11: Thermal conductivity of the different composite mixtures

Figure 12:

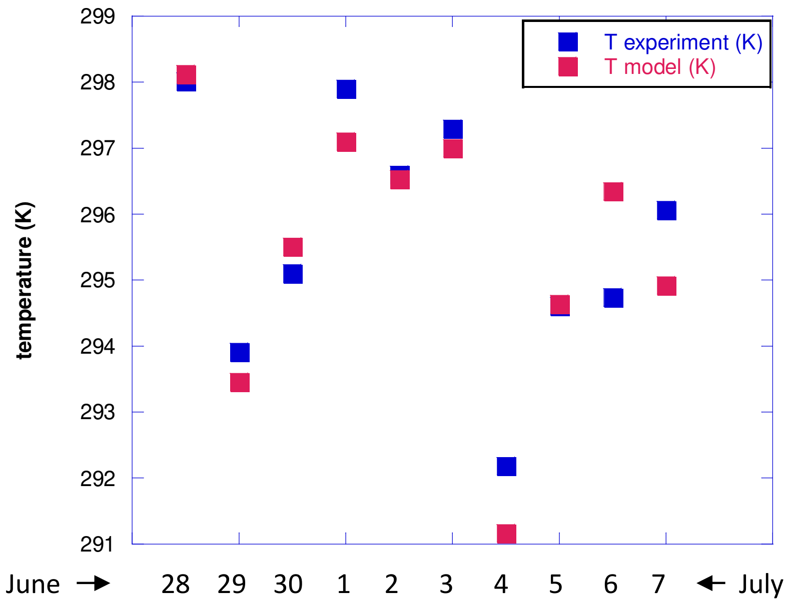

Fig. 12: Black globe temperature (K), model from OpenFOAM simulation (red squares) compared to experimental values (blue squares) for each day at 11 pm, during the period from June 28th to July 7th, 2011.

Figure 13:

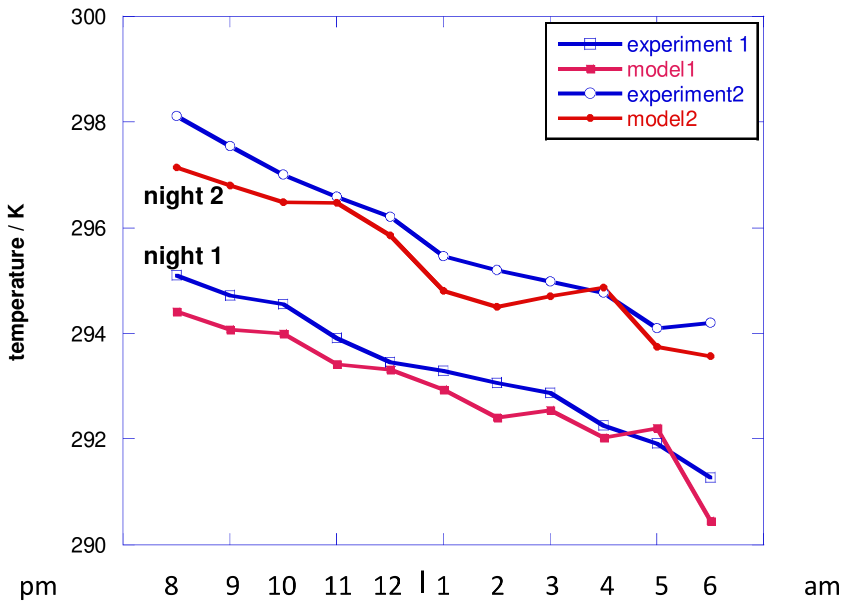

Fig. 13: Black globe temperatures (K) from OpenFOAM simulation (red curve) compared to experiment (blue curve), for the nights of June, 29th to 30th (night 1) and July 2nd to 3rd (night 2), 2011. The hours are from 8 pm to 6 am next day

Figure 14:

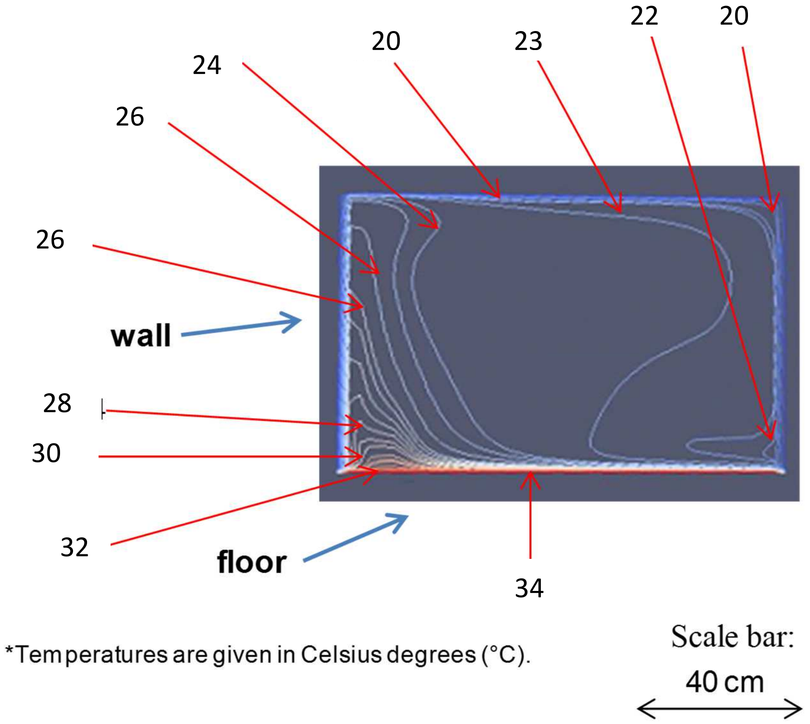

Fig. 14 : Field of temperature at 9 to 10 pm on July 2nd, 2011.

in red : hot floor temperature (34°C) ; in blue : ceiling and walls at external temperature (20.0°C).

Table 1. Thermal comfort zones with the corresponding enthalpy (H) values for piglets at different stages of life.

Animal phase	Lower critical temperature (°C)	Zone of thermal comfort				Higher critical temperature (°C)
		Minimum temperature (°C)	Minimum H (kJ/kg)*	Maximum temperature (°C)	Maximum H (kJ/kg)*	
Birth	15	32	84.0 – 90.6	34	88.6 – 95.9	35
1st week	13	28	75.5 – 80.7	32	84.0 – 90.6	35
2nd week	12	26	71.5 – 76.1	30	79.7 – 85.5	35
3rd week	10	24	67.6 – 71.7	26	71.5 – 76.1	35

(*) Enthalpy values for the 60-80% RH (relative humidity) range.

Adapted from: [4, 5, 8, 11-13].

Table 2. Formulations of the composites (% by dry mass)

Composites	Ordinary Portland cement	Deep bedding ashes	Sisal fiber	Sand	Water/binder ratio
Reference	25.0	-	-	75.0	0.50
OPC + DBA	17.2	7.4	-	75.4	0.65
OPC + Sisal	24.6	-	1.7	73.7	0.73
OPC + DBA + Sisal	17.2	7.4	1.7	73.7	1.30

Table 3. Composition of the multilayer board

Position	Thickness (cm)	Composites formulation (as in Table 2)
Top layer	1	OPC + DBA
Bottom layer	2	OPC + DBA + Sisal

Table 4. Thermal conductivities chosen as fixed entry data for the modeling

Material	Air	Insulating bricks	Insulating wood board	Ground
Thermal conductivity λ (W/ m K)	$2.63\ 10^{-4}$	0.7	0.1	0.0126

Table 5. Chemical composition (% by mass)

Oxides	Ordinary Portland cement (OPC)	Deep bedding ashes (DBA)
SiO_2	18.10	47.90
Al_2O_3	3.59	8.87
K_2O	1.13	7.79
Fe_2O_3	2.75	11.40
CaO	65.20	6.09
MgO	1.55	3.03
Na_2O	0.48	1.97
P_2O_5	0.17	8.13
TiO_2	0.27	2.58
SO_3	6.41	-
Cl	-	0.03
MnO	0.06	0.23
LOI *	0.00	6.51

(*) LOI: Loss on ignition

Table 6. Enthalpy calculation according to the air parameters registered at 11 pm.

Air parameters and enthalpy / Day	Day 1	Day 2	Day 3	Day 4
Air Temperature (°C)	14.51	20.41	22.18	23.10
Relative Humidity (RH%)	52.15	59.97	60.58	62.22
Enthalpy H (kJ/kg dry air)	48.64	58.58	61.62	63.50

Table 7: Validation of floor temperature modeling

Distance between the ground and the resistance of multilayer board (cm)	Experimental	Modeled 7.5	Modeled 6.5	Modeled 4.5
Multilayer board temperature (°C)	35.07	35.04	33.90	32.10

Table 8: Modeled temperatures (°C) compared to experimental counterparts at four different experimental dates

Period	Day 1		Day 2		Day 3		Day 4	
External temperature (°C)	8.79		15.29		17.84		18.51	
Multilayer board temperature (°C) *	E ** 29.19	M ** 31.13	E 32.20	M 33.77	E 32.95	M 34.73	E 33.99	M 35.77

(*) Temperature in the upper surface of the board

(**) E is for experimental temperatures and M for modeled temperatures.